Global Trends in Ocean Evaporation from Satellite Products

C. A. Clayson, S. Wijffels
Woods Hole Oceanographic Institution
and
J. B. Roberts, F. R. Robertson
NASA MSFC

2019 Joint Satellite Conference
Boston, MA
1 October 2019

Motivation

- Ocean evaporation is single largest component in global water cycle.
- Evaporation links water cycle to heat cycle through associated latent heat flux.
- Multiple analyses have demonstrated that *uncertainty* associated with evaporation is largest source of uncertainty in global water cycle.
- Expectations from long-term anthropogenic atmospheric warming are for an increase in global ocean evaporation over time.
- Improving our understanding of the global and regional trends in oceanic evaporation, and of the uncertainties in our current satellite datasets for analyzing these trends, is thus an important element towards understanding our global water and heat budgets.

Datasets

- Satellite
  - SeaFlux-v3: includes SSM/I, SSMIS, and other passive microwave data; OISST + diurnal SST; neural net retrievals of Qa, Ta, U
  - HOAPS 4.1: includes SSM/I, SSMIS. AVHRR-only OISST, uses 1D-Var scheme for wind speed; Qa is from Bentamy (2003) linear regression
  - IFREMER v4.1: winds combination of scatterometer retrievals; Qa retrieval dependent on SST, stability (from ICOADS and ERA-I).
  - J-OFURO3: winds combination of passive microwave and scatterometer; SST from ensemble of 12 analyses; Qa comes from SSM/I brightness temperatures plus information from integrated water vapor, ERA-I reanalysis.
- RedObs: Reanalyses that withhold satellite data: JRA55C, CERA-20C, NOAA ESRL 20CR
- OAFlux: assimilates buoys, satellite, ERA-I, ships
- ERA5

$$LHF = \rho L_v C_E U (Q_s - Q_a)$$

Area-averaged LHF anomalies

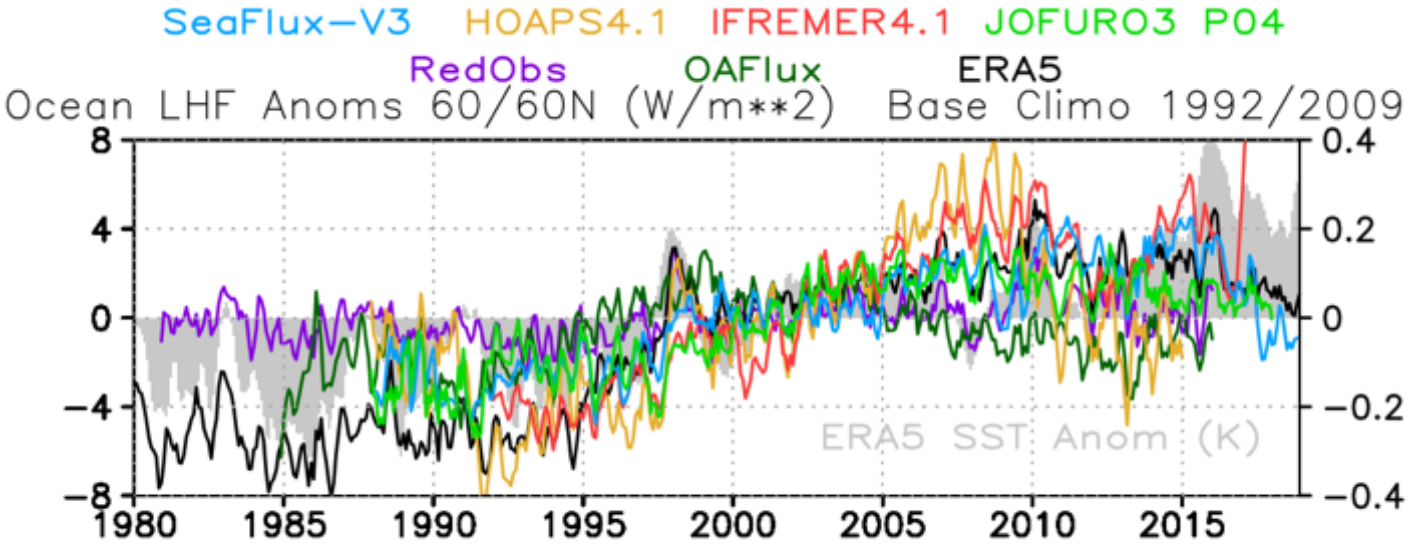

- Anomalies are from monthly resolved climatologies over 1992-2009 period.
- Solid gray shading is SST anomaly (°C)
- A running 3-month filter has been applied.

Robertson et al. 2019

Humidity trends

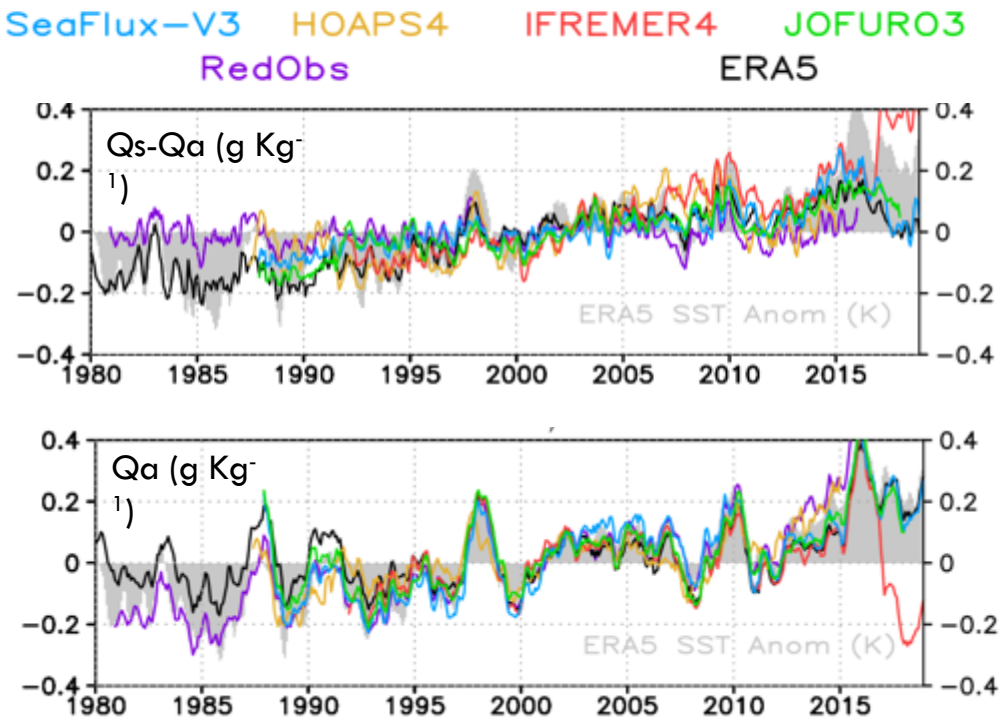

- Qa anomaly agreement among retrievals tracks global SST and highlights ENSO-driven variability.
- Poorer Qs-Qa agreement reflects both tight local control of SST on Qa as well as differences among SST data sets (e.g. AVHRR-only, blended passive microwave, reanalyses).

Robertson et al. 2019

Wind speed trends

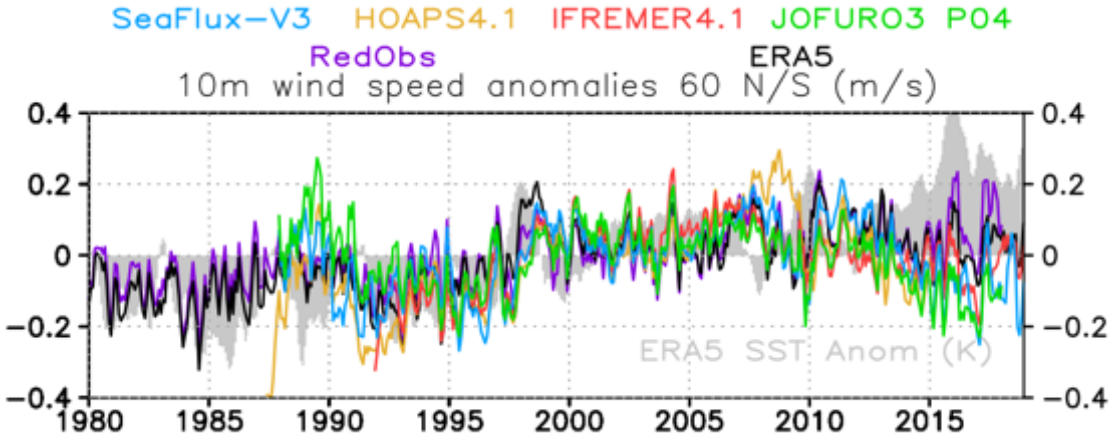

- Wind speed agreement poorer than Qa agreement
- Differences between satellite products increase in 2010s

SSMIS issues

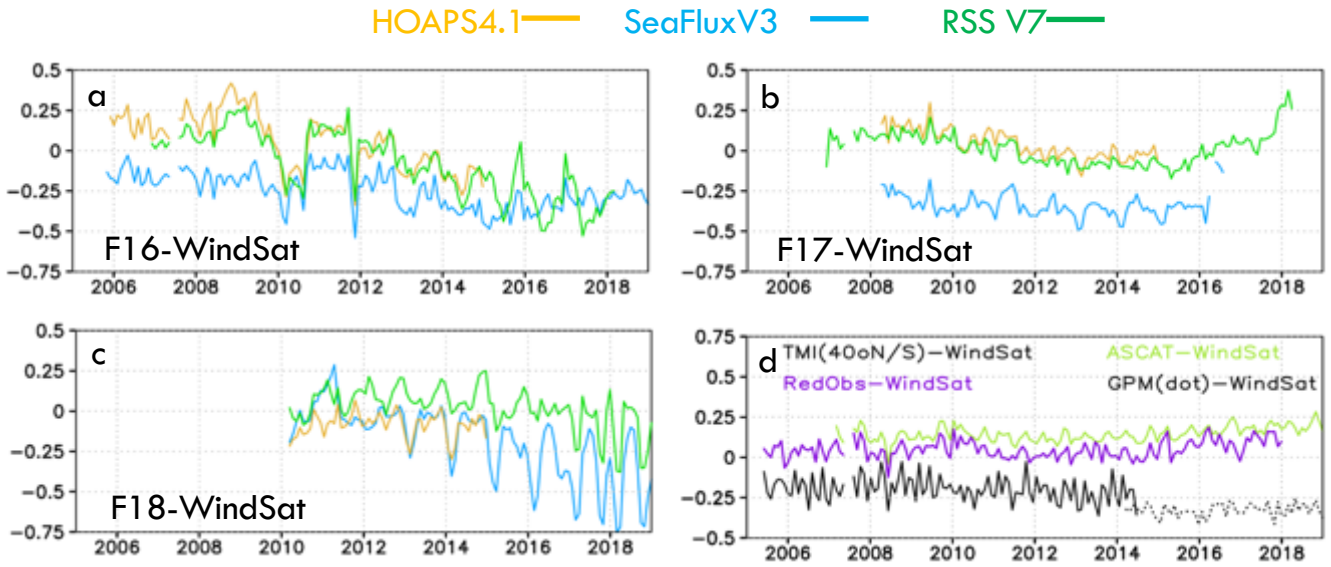

- Compared to WindSat, ASCAT, TMI/GMI and RedObs, the SSMIS sensors F16,F17,F18 have substantial *time-dependent* differences.

- Differences are present across retrieval algorithm (1DVAR and regression-based) and FCDR (i.e. GPM L1C, CM SAF, RSS) records

LHF trends (1992/1999 to 2000/2010)

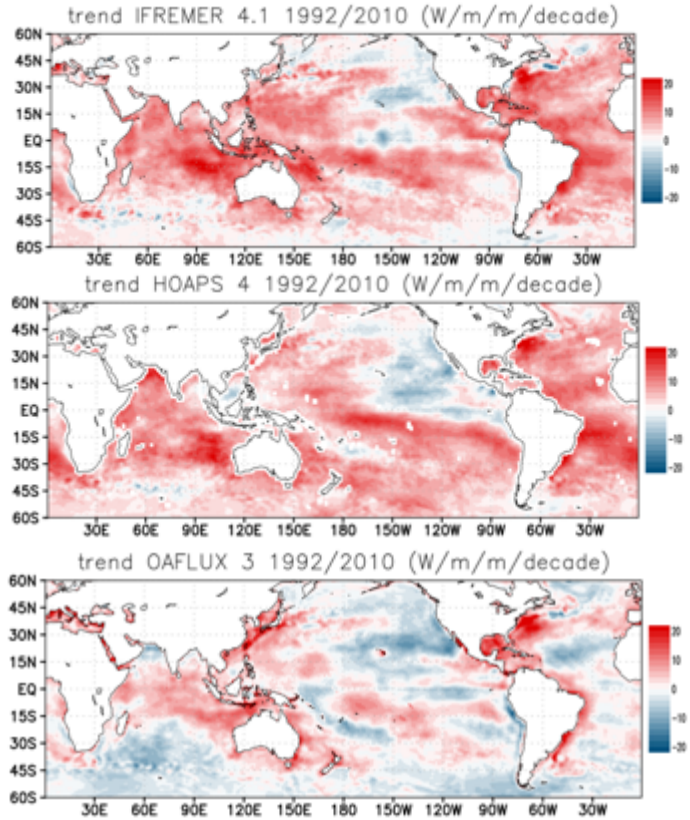

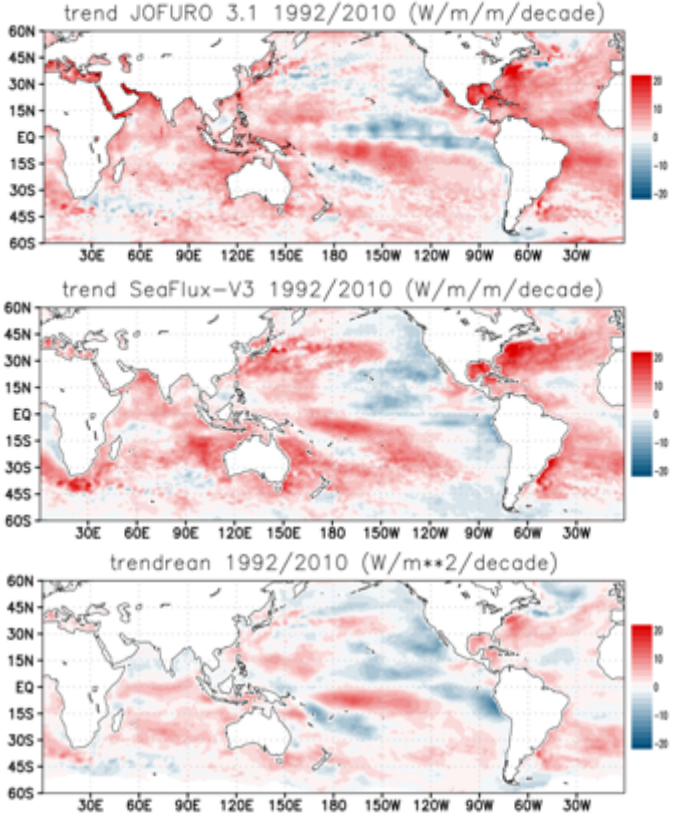

- All estimates indicate positive globally averaged trends but with downward trends over the eastern Pacific and within the SPCZ.
- IF4 and HO4 have systematically much larger trends than SFV3, JOF3 or RedObs owing to a combination of wind speed, qs(sst).
- JOF3 and IF4 show presence of TAO buoy data effects b/c they use ERA-I moisture data in their qa estimates.

Tropical Pacific LHF Trends

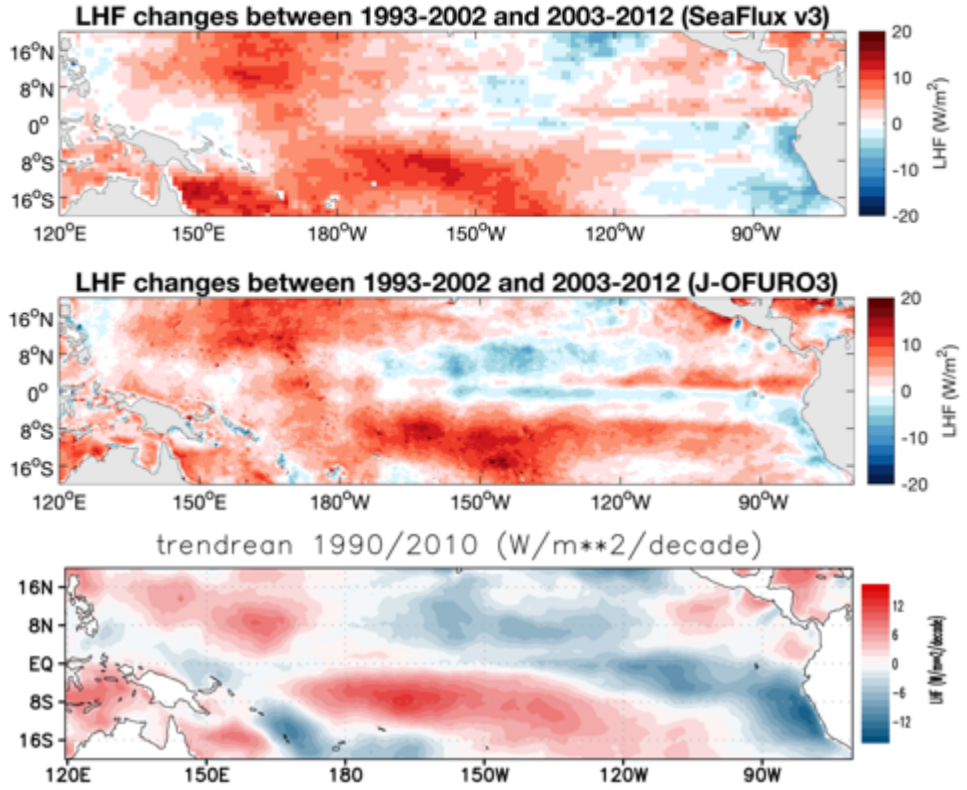

Temporal coverage of TAO buoys

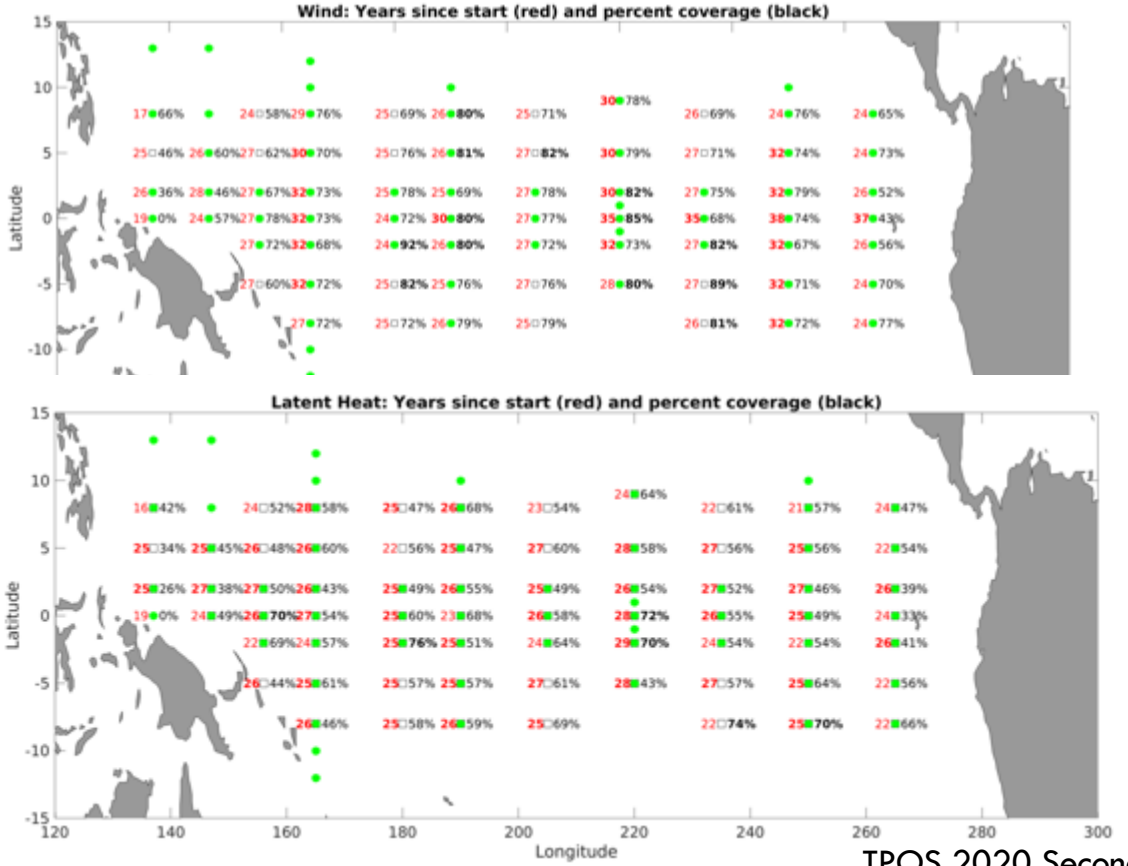

TPOS 2020 Second Report

Most complete buoy time series

- Buoy at 0°N, 156°E
- 26 year time record, 70% coverage
- Began operations 1992

Monthly Averaged LHF

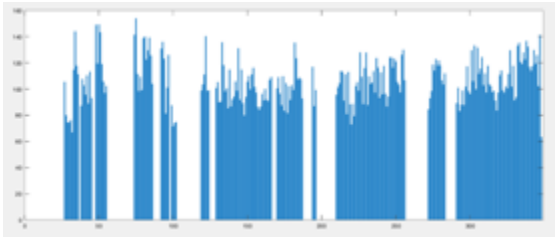

01/1990 12/2018

- Buoy at 2°S, 180°E
- 25 year time record, 76% coverage
- Began operations 11/1993

Monthly Averaged LHF

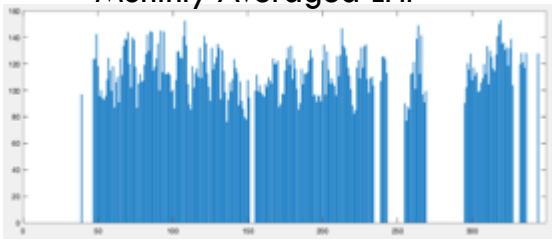

01/1990 12/2018

Tropical Pacific Variability

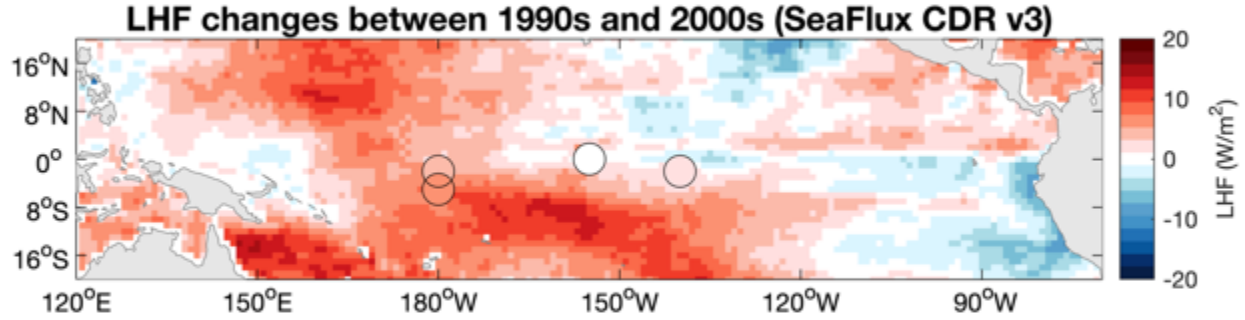

- Buoy monthly means only calculated for buoys with more than 70% data in a given month
- Buoy decadal values only calculated for buoys with more than 70% of the months

Means using available buoy data

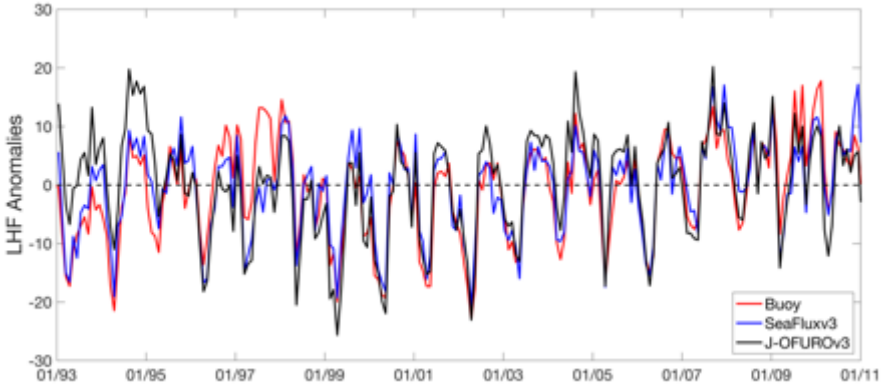

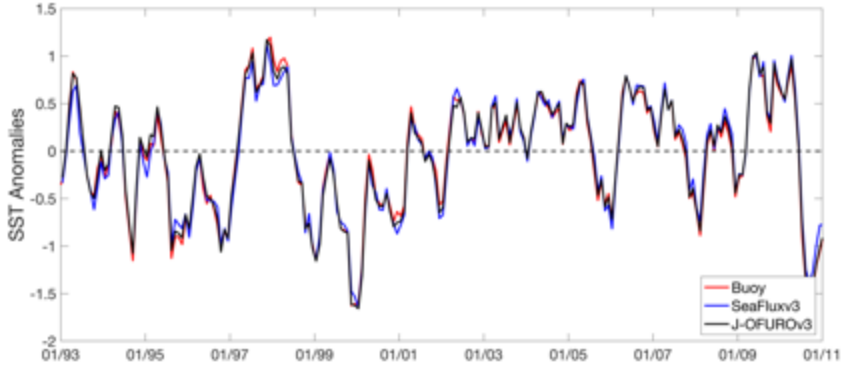

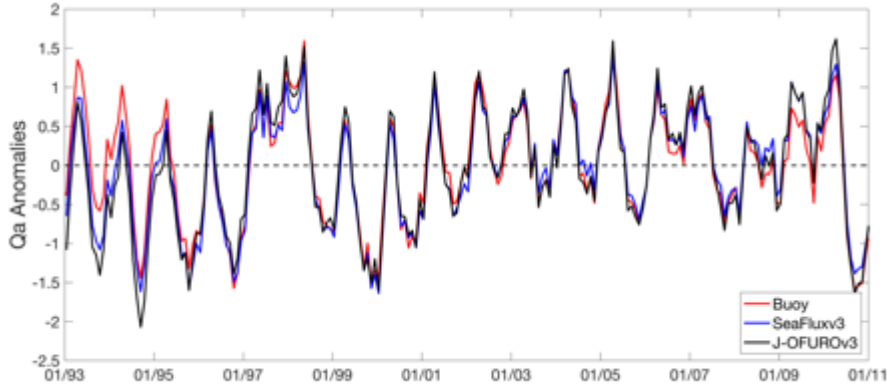

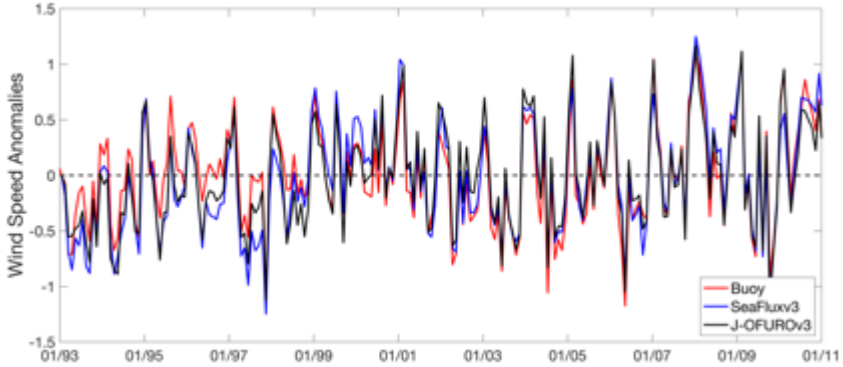

LHF cycles and trends from buoy data

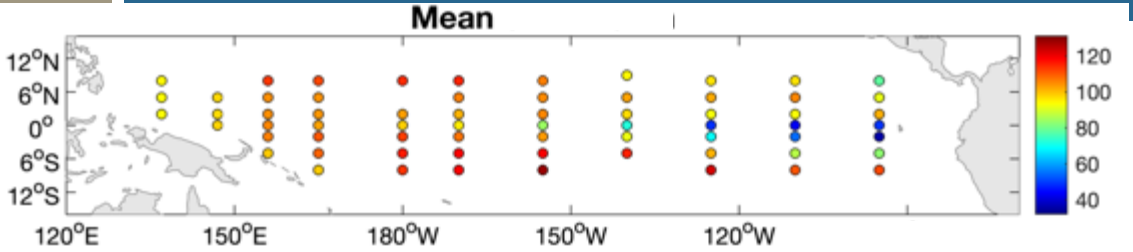

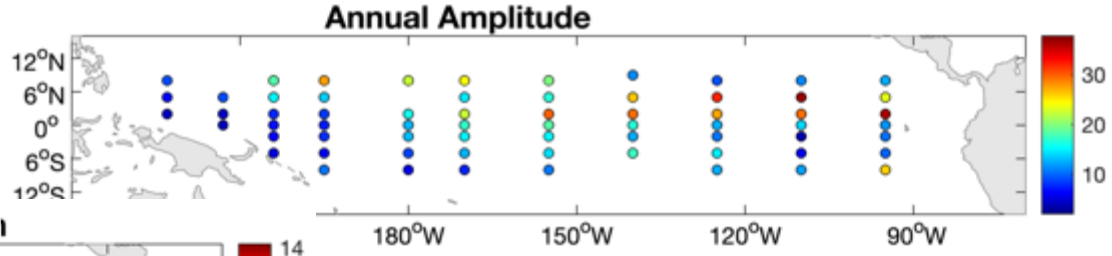

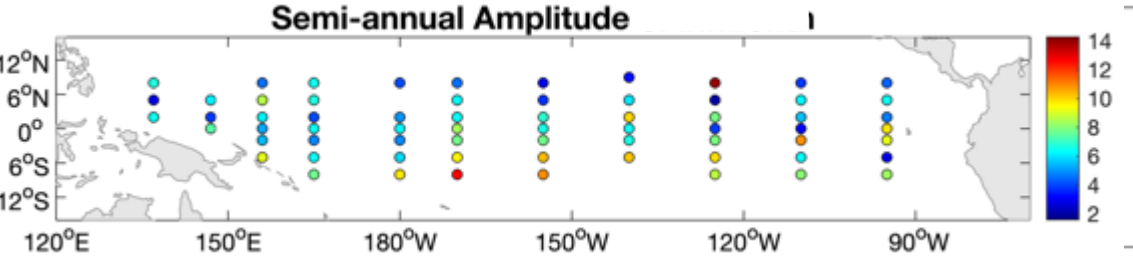

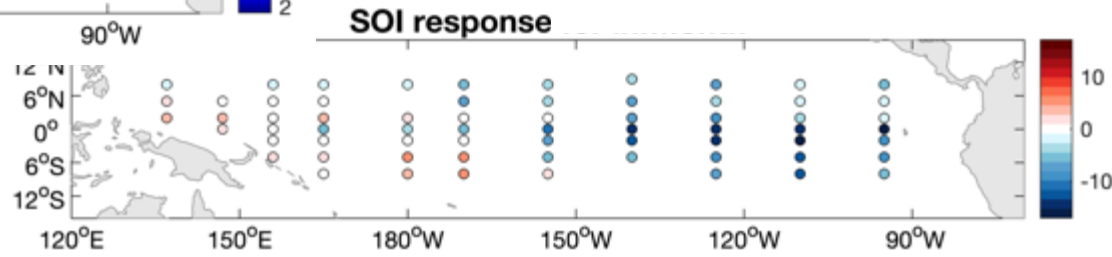

Reconstructed trend

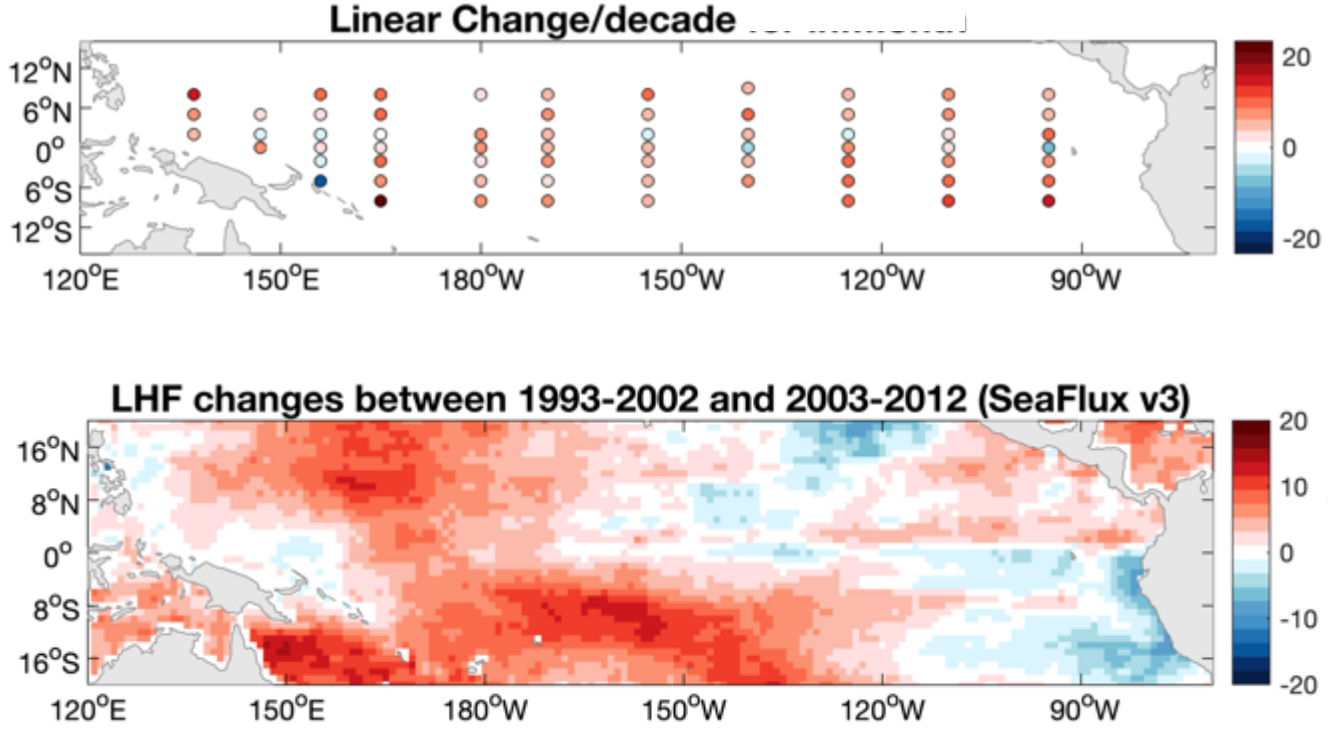

Errors correlated with dynamical regimes

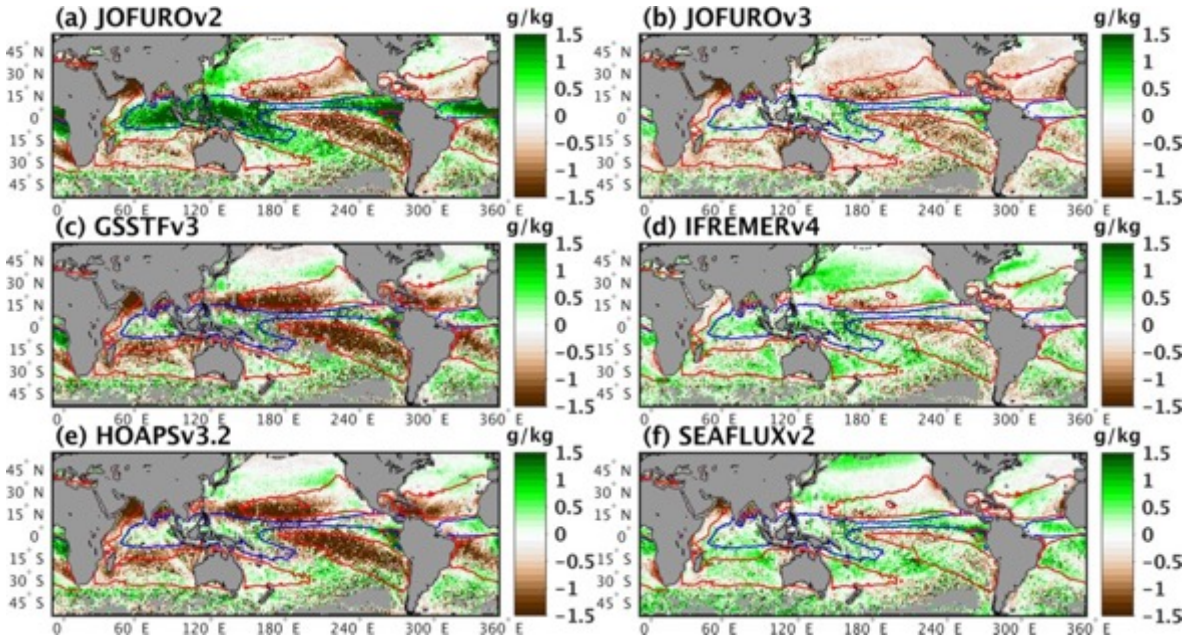

Figure 1. Mean differences (product minus observations) are shown for (a) JOFUROv2, (b) JOFUROv3, (c) GSSTFv3, (d) IFREMERv4, (e) HOAPSv3.2, and (f) SEAFLUXv2 over the common period 1999-2008. Red (blue) contours outline the 15% relative frequency of occurrence regions for the subtropical inversion layer/A0C- (deep convective/A0C+) dynamical regimes.

Roberts et al. 2019

Errors binned by dynamical regime

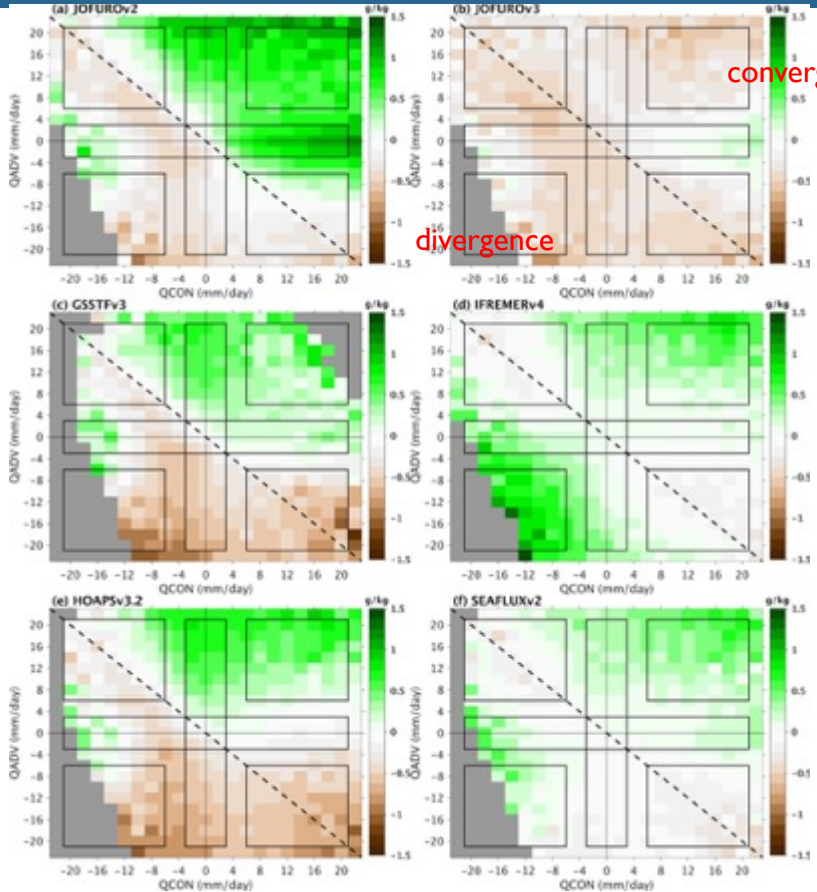

Roberts et al. 2019

Gains in consistency

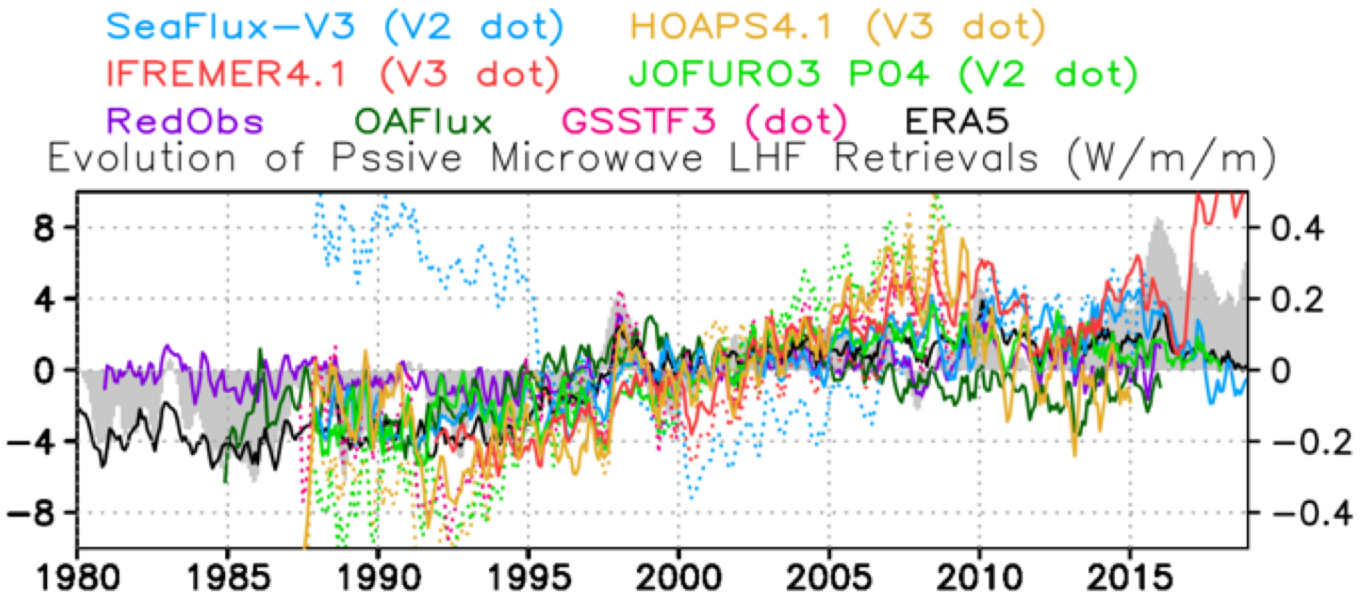

- Newer versions of datasets beginning to converge in global trends
- Improvements in datasets differ

Conclusions

- Continued convergence of satellite datasets in terms of global trends
- However:
  - Differences in trends remain across all components of bulk parameters, not just Qa (the usual suspect)
  - SSMIS issues affect products
  - Improvements vary between products
  - Switching of FCDRs without changes in algorithms proves problematic
- In situ datasets (i.e., buoys) can provide some information but data outages require very careful analysis to eliminate biasing
- Regime dependencies complicate understanding of trends across regions
  - Require ancillary data
  - Newer retrievals take dependencies into account: but reanalysis data used has its own set of trend issues
- Further comparisons with ocean assimilation data and salinity could help constrain E-P

FluxSat

Measuring air-sea heat and moisture fluxes from space

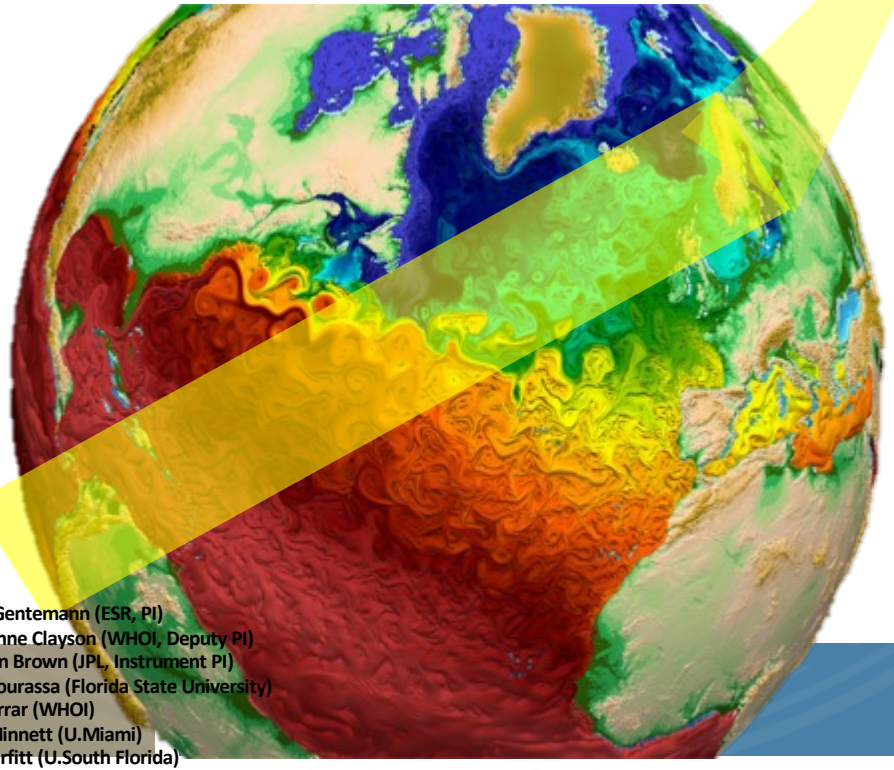

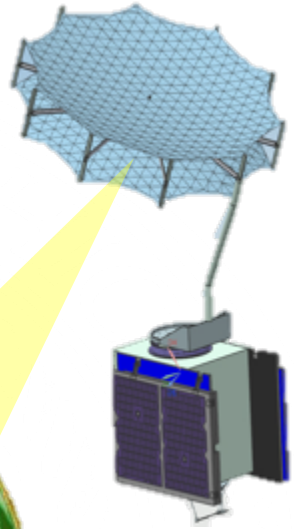

Small-sat passive microwave imager/sounder designed to measure air-sea flux

10km resolution sensible and latent heat flux over ocean

Resolve diurnal cycle

<2-day global coverage

Chelle Gentemann (ESR, PI)
Carol Anne Clayson (WHOI, Deputy PI)
Shannon Brown (JPL, Instrument PI)
Mark Bourassa (Florida State University)
Tom Farrar (WHOI)
Peter Minnett (U.Miami)
Rhys Parfitt (U.South Florida)